A Novel Molecular Beacon Bearing a Graphite Nanoparticle as a Nanoquencher for In Situ mRNA Detection in Cancer Cells.

ARTICLE *in* ACS APPLIED MATERIALS & INTERFACES · NOVEMBER 2012

Impact Factor: 6.72 · DOI: 10.1021/am301976r · Source: PubMed

3 AUTHORS, INCLUDING:

Yunxian Piao
Jilin University
17 PUBLICATIONS **204** CITATIONS
SEE PROFILE

Fei Liu
Stanford University
20 PUBLICATIONS **948** CITATIONS
SEE PROFILE

ACS APPLIED MATERIALS & INTERFACES

Research Article

www.acsami.org

A Novel Molecular Beacon Bearing a Graphite Nanoparticle as a Nanoquencher for In situ mRNA Detection in Cancer Cells

Yunxian Piao, Fei Liu, and Tae Seok Seo*

Department of Chemical and Biomolecular Engineering (BK21 program), Korea Advanced Institute of Science and Technology (KAIST), 291 Daehak-ro, Yuseong-gu, Daejeon 305-701, Republic of Korea

Supporting Information

ABSTRACT: Molecular beacons (MBs) have shown fascinating applications in many biological fields. However, exploration of cost-effective, sensitive, stable and efficient MB for in situ live cell- based assay has still room for improvement. In this regards, we have developed a novel MB which bears a spherical graphite nanoparticle (GN) as a fluorescent quencher. The GN resulted in the high quenching efficiency, and the presence of GN enhanced the biological stability and transfection of the MB into the cells, thereby enabling the real-time survivin mRNA detection and quantification in the MCF-7 breast cancer cells. These results demonstrated that the advancement of the proposed MB containing a GN nanoquencher can be used as a robust molecular probe for genetic analysis in the cells.

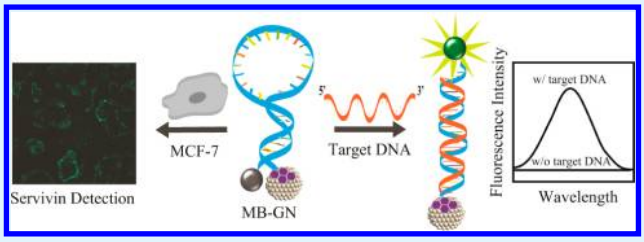

KEYWORDS: *graphite nanoparticle, molecular beacon, nanoquencher, FRET, survivin, breast cancer cell*

INTRODUCTION

Molecular beacons are hairpin-shaped oligonucleotides with a self-complementary stem that brings a fluorophore at one end and a quencher at the other end into close proximity, causing the fluorescence of the fluorophore to be quenched by energy transfer.[1] When there is a complementary target DNA, the MB spontaneously undergoes a conformational change with the stem opening and results in a fluorescence restoration. Due to the unique structural and thermodynamic properties, the MBs have been widely used in single nucleotide polymorphism detection,[2−4] pathogenic detection in real-time PCR,[5,6] and RNA gene expression within living cells.[7,8] Conventional MBs employ an organic dye as a fluorescent reporter and an organic moiety such as Dabcyl or BHQ as a quencher. To improve the detection sensitivity of the conventional MB, researchers have made several attempts by modifying either a donor fluorophore or an acceptor quencher.

Regarding the quencher modification, for example, Dubertret et al. employed a gold nanoparticle as a quencher for single base-mismatch detection by replacing Dabcyl with 1.4 nm gold clusters.[9] Yang et al. reported the use of a single-walled carbon nanotube as a quencher in the MB.[10] Metal-nanoquenchers such as gold nanoparticles[9,11,12] and silver nanoparticles[13] exhibited their superior quenching property, thereby improving detection sensitivity for DNA analysis, but they require a high-cost material preparation and tedious synthetic process to construct MB. In case of the nonmetallic quenchers such as carbon nanotube[10] and other carbon nanomaterials, they also proved excellent quenching efficiency, an economical synthetic method, and easy modification on the surface through the $\pi-\pi$ interaction with biomolecules. However, the lack of the controllability in their size and functional groups on the surface inevitably resulted in the limited reproducibility in the chemical and biological applications. Thus, it is worthwhile to explore further a novel fluorescent quencher that contains more desirable properties in terms of homogeneity, sensitivity, cost, and biological stability.

Recently, graphene, a single-layer of carbon atom in a closely packed honeycomb structure, has demonstrated not only extraordinary electronic properties,[14,15] but also fluorescence quenching characteristics in the bioassay.[16−20] Inspired from a series of reports related with the carbon-based quencher, herein, we propose a novel MB using a graphite nanoparticle (GN) as a quencher tag. GN is a spherical carbon nanomaterial with a diameter ranging from 4 to 5 nm, and consists of layer-by-layer stacked graphene sheets. Spherical morphology, a comparative size with the dye molecule, a graphene-like feature, and cost-effective synthesis endow the GN with an ideal fluorescence quencher in the MB.

EXPERIMENTAL SECTION

Materials. 6-carboxyfluorescein (FAM) and amino-modified hairpin oligonucleotides (5′-Amino-modifier-C6 spacer-CGACGGAGAAAGGGCTGCCACGTCG-FAM-3′), MB-Dabcyl (5′-Dabcyl-CGACGGAGAAAGGGCTGCCACGTCG-FAM-3′), and synthetic cDNA (5′-CTGCCTGGCAGCCCTTTCTCAAGGACCACCGCATCTCTACATTCAAGAAC-3′) were synthesized by Bioneer corporation (Korea). 1-Pyrenebutyric acid *N*-hydroxysuccinimide ester and deoxyribonuclease I (DNase I) were purchased from Sigma Aldrich (USA). Graphite nanoparticles were obtained from SkySpring Nanomaterials, Inc. (USA).

Received: September 13, 2012
Accepted: November 13, 2012
Published: November 13, 2012

   dx.doi.org/10.1021/am301976r | ACS Appl. Mater. Interfaces 2012, 4, 6785−6789

Synthesis and Characterization of the MB-Pyrene. The MB-pyrene was synthesized by reacting the FAM and amino-modified hairpin oligonucleotides (20 nmol) with 100-fold excess of 1-pyrenebutyric acid *N*-hydroxysuccinimide ester in a mixture of 40 μL of carbonate buffer (Na_2CO_3/$NaHCO_3$ pH 9.0) and 3 μL DMSO at room temperature overnight. The excess of 1-pyrenebutyric acid *N*-hydroxysuccinimide ester was removed by a size-exclusion chromatography on a PD-10 column, and then the produced MB-pyrene was purified by high-pressure liquid chromatography (HPLC) with a linear elution gradient of triethylammonium acetate in acetonitrile from 20 to 70% over 30 min. The collected fraction containing the MB-pyrene was vacuum-dried and stored at −20 °C until use. The HPLC was performed on a ProStat HPLC Station (Varian, CA) equipped with a photodiode array detector. The mass of the product was determined by using a matrix-assisted laser desorption/ionization time-of-flight (MALDI-TOF) mass spectrometry. Melting temperature measurements were conducted by using a real-time PCR thermocycler (Real-Time System, CFX Connect, Bio-Rad).

Synthesis and Characterization of the MB-GN Probe. The concentration of MB-pyrene was determined based on the 260 nm absorption band by using a UV−vis spectrophotometer (UV-2450, Shimadzu, Japan). The product solution was diluted with Mili-Q water to obtain the required concentration before use. 200 μg mL^{-1} of a GN solution suspended in water was reacted with 10 μM of an MB-pyrene aqueous solution for 2 h at room temperature. The insoluble GNs became homogeneous due to the attachment of MB-pyrene on the GN surface. The resultant MB-GN solution was centrifuged at 500 rpm for 1 h, and the impurities and the insoluble fraction of GNs were precipitated which were discarded. The supernatant containing the soluble MB-GN was collected and thoroughly washed with ultra-centrifugation at 13000 rpm. The unbound MB was removed from the supernatant and the precipitated MB-GN product was recovered and resuspended with Mili-Q water .

Cellular Experimental Procedures. Human breast cancer MCF-7 cells (Korean Cell Line Bank, Korea) were cultured in MEM media supplemented with 10% fetal bovine serum, 1% antibiotics, and 1 mM sodium pyruvate (all reagents from Gibco, Invitrogen) at 37 °C in an incubator equipped with a humidified atmosphere containing 5% CO_2. The proliferated MCF-7 cells were harvested with treatment of a 0.05% trypsin solution. 5 × 10^4 cells were plated in the 8-well chambered coverslides and placed in the CO_2 incubator for 1 day. Then, the media was replaced with new one which contains 4.4 μM MB-Dabcyl or MB-GN probes. After incubation for 12 h at 37 °C, the cell medium was decanted from the well, and the cells were washed thoroughly with a cell culture grade PBS. The fluorescence image was conducted by a confocal microscope (Nikon, D-ECLIPSE, C1si). For up-regulating survivin mRNA expression, the MCF-7 cells were treated with 0, 20, 50, 80, 100, and 150 nM of docetaxel for 24 h, and the fluorescence image of the cells was monitored by a confocal microscopy. For cytotoxicity test, MCF-7 cells were incubated with various concentrations of GN in a CO_2 incubator at 37 °C for 24 h, and the relative cell viability was obtained by using LIVE/DEAD viability/cytotoxicity kit (Molecular Probes, Invitrogen).

RESULTS AND DISCUSSION

We synthesized a novel MB modified with GN (MB-GN) as shown in Figure 1. First, the MB having a FAM dye at the 3′ end and an amino group at the 5′ end has reacted with 1-pyrenebutyric acid *N*-hydroxysuccinimide ester to attach a pyrene functional group at the 5′ end. After purification with HPLC, the pyrene conjugate was confirmed by observing the major single peak at 8758 m/z (theoretical value: 8761 m/z) in the matrix-assisted laser desorption/ionization time-of-flight mass spectrometry analysis (see Figure S1 in the Supporting Information). Then, the pyrene group in the MB was used for linking the GN through the $\pi-\pi$ stacking mechanism. To confirm such a π-stacking mediated conjugation, we incubated the pyrene with a GN solution. After a thorough washing step,

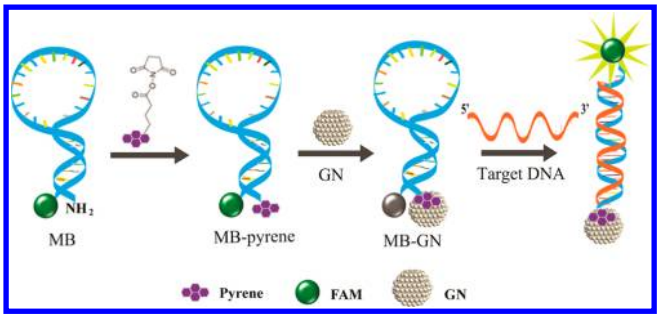

Figure 1. Schematics for the synthesis of an MB-GN and its application for target gene detection. An amino-modified MB was conjugated with a pyrene moiety which attaches a GN through $\pi-\pi$ stacking. Once the GN is labeled, the fluorescence signal of FAM fluorophore (a donor) is quenched by the GN (an acceptor) by FRET phenomenon. When a target DNA is hybridized with the MB, the FAM signal was recovered.

the conjugation of pyrene with GN was investigated by UV−vis absorption spectroscopy, and the unique absorption peaks of pyrene were revealed at 240, 264, 274, 322, and 341 nm, demonstrating the π-stacking between the pyrene and GN (see Figure S2 in the Supporting Information). The GN was also characterized by the Raman spectra, and displayed the typical graphite crystalline property by showing G band at 1578 cm^{-1} and D band at1355 cm^{-1} . The intensity of the D peak is relatively large probably due to the defects of the crystal edges generated from the assembly of the different sizes of multiple graphene sheets, revealing that the intensity ratio of D to G is 0.86.[21−23]

Because the double-stranded stem part does not join the $\pi-\pi$ interaction with the GN and the pyrene is a stronger moiety than the base of nucleotides for stacking on the graphene surface,[24−26] it would be expected that the GN is mainly conjugated with the MB through the pyrene group. After washing with centrifugation at 13 000 rpm, the final MB-GN product which has a FAM at the 3′ end and the GN at the 5′ end was recovered from the supernatant. Without a target DNA, the FAM fluorophore is placed on the GN surface in close proximity that results in the quenching of FAM signal by the nonradiative energy transfer from FAM (a donor) to GN (an acceptor). Once hybridized with a target DNA, the FAM is separated from the GN, restoring its fluorescence signal.

Figure 2A shows the UV−vis absorption spectra of the MB-pyrene and MB-GN. The pyrene modified MB represents distinct absorption maxima at 260 nm by DNA, at 322 and 341 nm by pyrene, and at 450 and 490 nm by FAM. The MB-GN revealed a broad peak around 260 nm that was absent from the pristine GN, suggesting a successful conjugation of MB DNA on the GN surface. However, the absorption peaks of pyrene and FAM were suppressed because of the GNs. Comparison of the TEM image in Figure 2B, C shows that the clear boundary of the pristine GN became smeared because of MB on the GN surface. The inset of Figure 2B shows an isolated GN that shows a growth ring pattern due to the multistacking of the graphene sheets.

We evaluated the capability of the GN as a nanoquencher for the fluorescent dye, and investigated the ability of the as-synthesized MB-GN probe for monitoring mRNA gene expression in the live cells. First, we performed the hybridization reaction between the MB-GN (5′-GN-CGACGGAGAAAGGGCTGCCAC-GTCG-FAM) and a synthetic cDNA (5′-CTGCCTGGCAGCCC-TTTCTCAAGGACCACCGCATCTCTACATTCAAGAAC-3′)

dx.doi.org/10.1021/am301976r | ACS Appl. Mater. Interfaces 2012, 4, 6785−6789

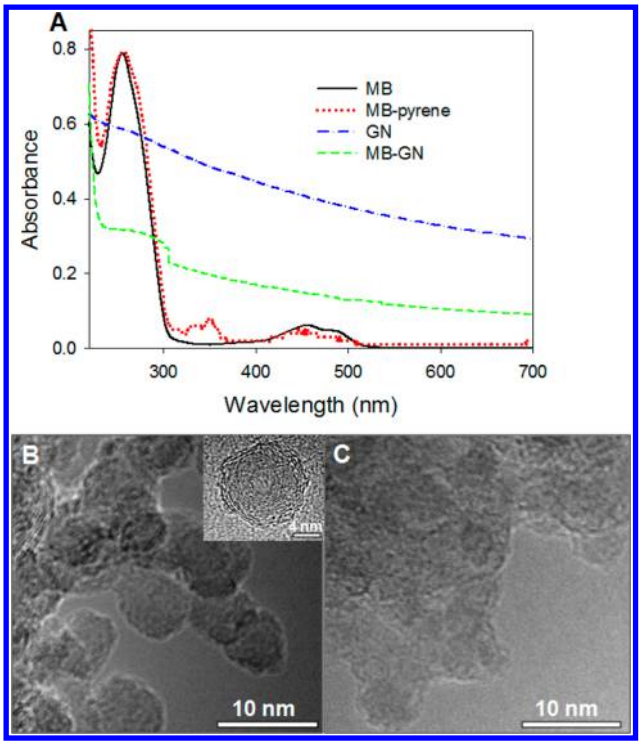

Figure 2. (A) UV−vis absorption spectra of the MB-pyrene and MB-GN. TEM images of GN (B) before and (C) after conjugation with a pyrene labeled MB. The inset in (B) shows an isolated single GN, which displays a multistacking graphene sheets in order.

in which the target cDNA sequence was determined by mimicking survivin gene. Figure 3 shows the change of the fluorescence signal

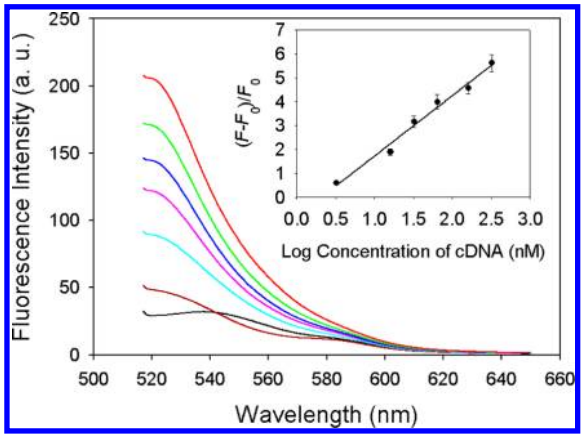

Figure 3. Fluorescence emission spectra of the MB-GN without cDNA and upon the addition of cDNA with log concentration at 0.5, 1.2, 1.5, 1.8, 2.2, and 2.5 (from bottom to top). Inset: a linear relationship between the relative fluorescence intensity and the logarithm of cDNA concentration. Error bars were obtained from three separate experiments.

before and after hybridization. The initial fluorescence intensity of MB-GN was minimal, indicating the efficient fluorescent quenching by a GN tag. Once the target cDNA was hybridized with the complementary loop sequence of MB, the fluorescent signal was gradually recovered as the concentration of cDNA was increased. The relative fluorescence intensity, $(F - F_0)/F_0$ where F_0 and F are the fluorescence intensity without and with the presence of cDNA, was linearly proportional to the logarithm of cDNA concentration ranging from 0.5 to 2.5 nM. The correlation equation was obtained as $y = 1.09x - 0.7641$ ($R^2 = 0.9837$) and the limit of detection was 3 nM.

We compared the quenching efficiency of GN with that of the organic Dabcyl quencher. Under the same conditions, the quenching efficiency of GN was estimated as 97.7 ± 1.9%, whereas that of the Dabcyl was 87.53 ± 5.7%, showing 11% improvement of GN over the Dabcyl quencher (see Figure S4 in the Supporting Information). These results present that the MB-GN retains the functionality of stem-loop structure and the hybridization event efficiently separates the fluorophore from the GN quencher, demonstrating a success of a novel molecular beacon probe with GN. One of the drawbacks of the conventional MB is that it has tendency to be cleaved off by nuclease enzyme, limiting its application in the live cell based assay.[27] We hypothesized that the presence of the GN can provide the MB with good resistance toward nuclease cleavage activity. To prove this hypothesis, we performed in vitro digestion experiments by reacting 35 pmol of conventional MB-Dabcyl and MB-GN with 1 U DNase I which can nonspecifically cleave single-stranded and double-stranded DNA. After 2 h of incubation at room temperature, the fluorescence signal of the conventional MB-Dabcyl increased by 145-fold over the DNase I nontreated one (Figure 4), showing the conventional MB is significantly

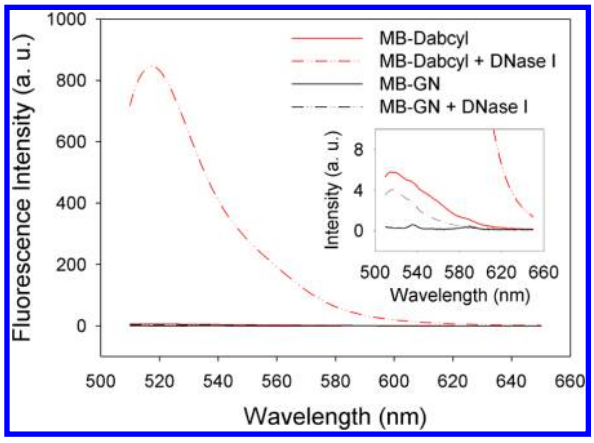

Figure 4. Fluorescence emission spectra of a conventional MB-Dabcyl and MB-GN before and after reaction with DNase I.

labile to the nuclease enzyme. On the other hand, under the identical experimental conditions, the MB-GN probe displayed only 15-fold fluorescence enhancement (inset in Figure 4). These results suggest that the DNA in the MB-GN is well protected from the nuclease enzyme activity, and the steric hindrance derived from the conjugated GN may prevent the DNase I from accessing to MB-GN. In addition, the thermal stability of the MB-GN was investigated by melting temperature measurements (see Figure S5 in the Supporting Information). Because of the strong binding affinity between the MB and the GN, the fluorescence intensity was negligible regardless of the increase of temperature, meaning the high thermal stability of the MB-GN. However, when the target DNA was incubated together with the MB-GN, the fluorescence signal of the MB-GN was significantly improved. As the temperature increased from 25 to 80 °C, the fluorescence intensity was gradually reduced. This result may be due to the fact that the target DNA was dehybridized at high temperature and the resultant flexible single-stranded MB would place the FAM close to the GN with

dx.doi.org/10.1021/am301976r | ACS Appl. Mater. Interfaces 2012, 4, 6785−6789

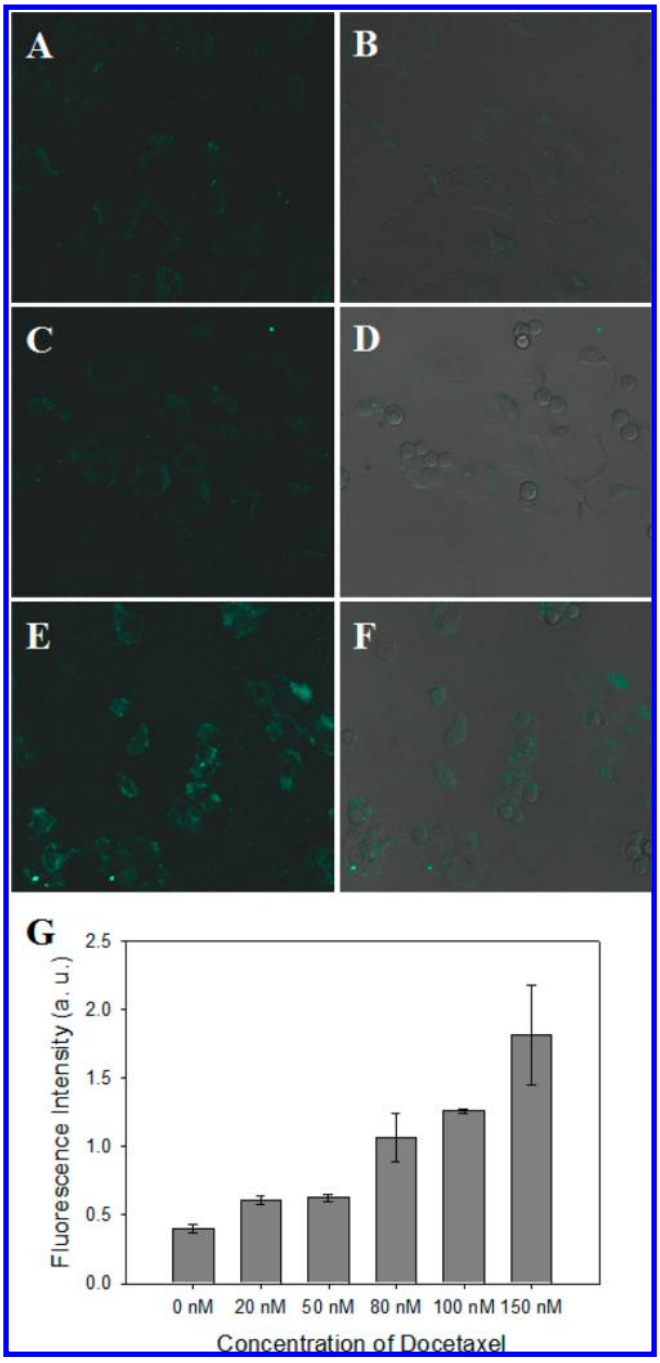

Figure 5. Monitoring of the survivin gene expression level in the viable cells by using MB-GN probes. Confocal fluorescence images of MCF-7 cells treated with variation of docetaxel concentration: (A, B) no docetaxel treatment, (C, D) 20 nM docetaxel treated, and (E, F) 100 nM docetaxel treated. (left panel) FAM fluorescence image and (right panel) bright-field and fluorescence-field merged image. (G) Quantitative analysis of fluorescence intensity depending on the docetaxel concentration.

higher probability than the double stranded MB-target DNA hybrid at lower temperature.

Taking full advantages of the high fluorescence quenching efficiency, the strong nuclease resistance and thermal stability of the as-synthesized MB-GNs, we utilized them for detecting in situ mRNA in live cells. The human breast cancer MCF-7 cells, which express survivin transcripts, were used as a model. The loop sequence of an MB was designed as reported, which selectively targets mRNA of survivin that is considered as a potential marker in cancer therapeutics and diagnostics.[28,29] Since the nanoparticles are reported to be well uptaken by cells through endocytosis mechanism, the transfection efficiency of the MB-GN into the cells should be better than the conventional MB. A 4.4 μM of the MB-GN probe was incubated with 5×10^4 MCF-7 cells at 37 °C for 12 h, allowing the probe to be translocated across the cell membrane and be delivered to the cells. Upon encountering with a target mRNA in cytosol, the MB structure will be open to place the FAM dye apart from the GN quencher, leading to fluorescence restoration which was monitored by a confocal microscopy. When MCF-7 cells were treated with MB-GN probes, higher fluorescence signal was observed in most of the cells than the conventional MB because of the efficient MB delivery and survivin mRNA targeting of the MB-GN (see Figure S6-A, C in the Supporting Information). These results proved that the high biological stability and high transfection efficiency make the MB-GN an ideal nanoprobe for in vivo cell imaging. To investigate whether the MB-GN survivin probe can monitor the level of real-time mRNA expression in viable cells, we stimulated the MCF-7 cells with docetaxel, which can up-regulate survivin gene expression. After MCF-7 cells were transfected with the MB-GN, they were treated with docetaxel for 24 h. The intensity of the green fluorescence was gradually increased in proportion to the concentration of docetaxel (Figure 5A–F). The relative level of survivin mRNA could be quantified by calculating the average fluorescence intensity per unit area (μm^2) in the cells. It turns out that the treatment with 20, 50, 80, 100, and 150 nM docetaxel resulted in about 1.52, 1.56, 2.67, 3.14, and 4.53-fold fluorescence intensity enhancement, respectively, in comparison with the pristine survivin gene level of MCF-7 cells (Figure 5G). In addition, we evaluated the cytotoxicity of MB-GN with concentration range from 1 to 1000 μg/mL (see Figure S7 in the Supporting Information).- About 90% of the cell viability was maintained even when the GN concentration of 1000 μg/mL was used, thereby demonstrating the low cytotoxicity of MB-GN and its usefulness as a nanoprobe for mRNA gene expression in the cells. Compared with other carbon nanoprobe-based cell detection, the MB-GN shows lower cytotoxicity, comparable transfection efficiency, and a longtime cell imaging.[16,30]

These results strongly imply that the novel MB-GN probe can be not only used for mRNA detection in live cancer cells with high stability and reliability, but also can real-time monitor gene expression quantitatively.

CONCLUSIONS

We have developed a novel MB by using a spherical graphite nanoparticle as a fluorescent quencher, and demonstrated its advantages as a molecular probe such as low cost, facile conjugation, strong nuclease resistance, high thermostability, and transfection ability. Because of these characteristics, we could successfully image the target survivin mRNA inside the cancer cells and furthermore monitor gene expression variation depending on the stimulant concentration. This novel MB coupled with GN can expand its application arena to many biological fields including gene and protein analysis, and drug screening.

ASSOCIATED CONTENT

Supporting Information

MALDI-TOF mass data for the synthesized MB-pyrene conjugate, UV–vis absorption spectra of GN before and after pyrene conjugation, Raman spectrum of the GN, fluorescence emission spectra of the MB-GN and MB-Dabcyl, thermodynamic

property of the MB-GN, cell imaging by using the MB-GN and MB-Dabcyl probes, and relative cell viability of MCF-7 cells after incubation with various concentrations of the GN. This material is available free of charge via the Internet at http://pubs.acs.org.

AUTHOR INFORMATION

Corresponding Author

*E-mail: seots@kaist.ac.kr.

Notes

The authors declare no competing financial interest.

ACKNOWLEDGMENTS

This work was supported by the Basic Science Research Program through the National Research Foundation of Korea (NRF) funded by the Ministry of Education, Science and Technology (2012-0004343), the Converging Research Center Program funded by the Ministry of Education, Science and Technology (2011K000837), and the Converging Technology Project funded by the Korean Ministry of Environment (M112-00061-0002-0).

REFERENCES

(1) Tyagi, S.; Kramer, F. R. *Nat. Biotechnol.* **1996**, *14*, 303−308.
(2) Piatek, A. S.; Tyagi, S.; Pol, A. C.; Telenti, A.; Miller, L. P.; Kramer, F. R.; Alland, D. *Nat. Biotechnol.* **1998**, *16*, 359−363.
(3) Kostrikis, L. G.; Tyagi, S.; Mhlanga, M. M.; Ho, D. D.; Kramer, F. R. *Science* **1998**, *279*, 1228−1229.
(4) Tyagi, S.; Bratu, D. P.; Kramer, F. R. *Nat. Biotechnol.* **1998**, *16*, 49−53.
(5) Karge, W. H., 3rd; Schaefer, E. J.; Ordovas, J. M. *Methods Mol. Biol.* **1998**, *110*, 43−61.
(6) Jung, R.; Soondrum, K.; Neumaier, M. *Clin. Chem. Lab. Med.* **2000**, *38*, 833−836.
(7) Bratu, D. P.; Cha, B. J.; Mhlanga, M. M.; Kramer, F. R.; Tyagi, S. *Proc. Natl. Acad. Sci. U.S.A.* **2003**, *100*, 13308−13313.
(8) Mhlanga, M. M.; Vargas, D. Y.; Fung, C. W.; Kramer, F. R.; Tyagi, S. *Nucl. Acids Res.* **2005**, *33*, 1902−1912.
(9) Dubertret, B.; Calame, M.; Libchaber, A. J. *Nat. Biotechnol.* **2001**, *19*, 365−370.
(10) Yang, R.; Jin, J.; Chen, Y.; Shao, N.; Kang, H.; Xiao, Z.; Tang, Z.; Wu, Y.; Zhu, Z.; Tan, W. *J. Am. Chem. Soc.* **2008**, *130*, 8351−8358.
(11) Yang, C. Y. J.; Lin, H.; Tan, W. H. *J. Am. Chem. Soc.* **2005**, *127*, 12772−12773.
(12) Maxwell, D. J.; Taylor, J. R.; Nie, S. *J. Am. Chem. Soc.* **2002**, *124*, 9606−9612.
(13) Jaiswal, A.; Sanpui, P.; Chattopadhyay, A.; Ghosh, S. S. *Plasmonics* **2011**, *6*, 125−132.
(14) Geim, A. K.; Novoselov, K. S. *Nat. Mater.* **2007**, *6*, 183−191.
(15) Liu, F.; Piao, Y.; Choi, K. S.; Seo, T. S. *Carbon* **2012**, *50*, 123−133.
(16) Lu, C. H.; Zhu, C. L.; Li, J.; Liu, J. J.; Chen, X.; Yang, H. H. *Chem. Commun.* **2010**, *46*, 3116−3118.
(17) Piao, Y.; Liu, F.; Seo, T. S. *Chem. Commun.* **2011**, *47*, 12149−12151.
(18) Huang, P.-J. J.; Liu, J. *Anal. Chem.* **2012**, *84*, 4192−4198.
(19) Liu, F.; Choi, J. Y.; Seo, T. S. *Biosens. Bioelectron.* **2010**, *25*, 2361−2365.
(20) Jung, J. H.; Cheon, D. S.; Liu, F.; Lee, K. B.; Seo, T. S. *Angew. Chem., Int. Ed.* **2010**, *49*, 5708−5711.
(21) Nemanich, R. J.; Solin, S. A. *Phys. Rev. B* **1979**, *20*, 392−401.
(22) Kim, H.-M.; Kim, K.-M.; Lee, K.; Kim, Y. S.; Oh, J.-M. *Eur. J. Inorg. Chem.* **2012**, 5343−5349.
(23) Li, Y.; Zhao, Y.; Cheng, H.; Hu, Y.; Shi, G.; Dai, L.; Qu, L. *J. Am. Chem. Soc.* **2012**, *134*, 15−18.
(24) Lee, D.-W.; Kim, T.; Lee, M. *Chem. Commun.* **2011**, *47*, 8259−8261.
(25) Zhang, M.; Parajuli, R. R.; Mastrogiovanni, D.; Dai, B.; Lo, P.; Cheung, W.; Brukh, R.; Chiu, P. L.; Zhou, T.; Liu, Z.; Gar-funkel, E.; He, H. *Small* **2010**, *6*, 1100−1107.
(26) Chen, Q.; Wei, W.; Lin, J.-M. *Biosens. Bioelectron.* **2011**, *26*, 4497−4502.
(27) Chen, A. K.; Behlke, M. A.; Tsourkas, A. *Nucl. Acids Res.* **2007**, *35*, e105.
(28) Peng, X. H.; Cao, Z. H.; Xia, J. T.; Carlson, G. W.; Lewis, M. M.; Wood, W. C.; Yang, L. *Cancer Res.* **2005**, *65*, 1909−1917.
(29) Altieri, D. C. *Oncogene* **2003**, *22*, 8581−8589.
(30) Wu, Y.; Phillips, J. A.; Liu, H.; Yang, R.; Tan, W. *ACS Nano* **2008**, *2*, 2023−2028.